British Journal of Pharmacology

DOI:10.1111/bph.12991
www.brjpharmacol.org

Themed Section: Chinese Innovation in Cardiovascular Drug Discovery

RESEARCH PAPER

Regulator of G-protein signalling 5 protects against atherosclerosis in apolipoprotein E-deficient mice

Wen-Lin Cheng[1], Pi-Xiao Wang[2,3], Tao Wang[2,3], Yan Zhang[2,3], Cheng Du[2,3], Hongliang Li[2,3] and Yong Ji[1]

[1]*Key Laboratory of Cardiovascular Disease and Molecular Intervention, Key Laboratory of Human Functional Genomics, Atherosclerosis Research Centre, Nanjing Medical University, Nanjing, China,* [2]*Department of Cardiology, Renmin Hospital of Wuhan University, Wuhan, China, and* [3]*Cardiovascular Research Institute, Wuhan University, Wuhan, China*

Correspondence
Yong Ji, Key Laboratory of Cardiovascular Disease and Molecular Intervention, Key Laboratory of Human Functional Genomics, Atherosclerosis Research Centre, Nanjing Medical University, Hanzhong Road 140, Nanjing 210029, China. E-mail: yongji@njmu.edu.cn
Hongliang Li, Department of Cardiology, Renmin Hospital of Wuhan University, Cardiovascular Research Institute, Wuhan University, Jiefang Road 238, Wuhan 430060, China. E-mail: lihl@whu.edu.cn

Yong Ji and Hongliang Li contribute equally.

Received
10 June 2014
Revised
21 October 2014
Accepted
24 October 2014

BACKGROUND AND PURPOSE

Atherosclerosis is a chronic inflammatory disease, in which 'vulnerable plaques' have been recognized as the underlying risk factor for coronary disease. Regulator of G-protein signalling (RGS) 5 controls endothelial cell function and inflammation. In this study, we explored the effect of RGS5 on atherosclerosis and the potential underlying mechanisms.

EXPERIMENTAL APPROACH

RGS5$^{-/-}$ apolipoprotein E (ApoE)$^{-/-}$ and ApoE$^{-/-}$ littermates were fed a high-fat diet for 28 weeks. Total aorta surface and lipid accumulation were measured by Oil Red O staining and haematoxylin–eosin staining was used to analyse the morphology of atherosclerotic lesions. Inflammatory cell infiltration and general inflammatory mediators were examined by immunofluorescence staining. Apoptotic endothelial cells and macrophages were assayed with TUNEL. Expression of RGS5and adhesion molecules, and ERK1/2 phosphorylation were evaluated by co-staining with CD31. Expression of mRNA and protein were determined by quantitative real-time PCR and Western blotting respectively.

KEY RESULTS

Atherosclerotic phenotypes were significantly accelerated in RGS5$^{-/-}$ApoE$^{-/-}$ mice, as indicated by increased inflammatory mediator expression and apoptosis of endothelial cells and macrophages. RGS5 deficiency enhanced instability of vulnerable plaques by increasing infiltration of macrophages in parallel with the accumulation of lipids, and decreased smooth muscle cell and collagen content. Mechanistically, increased activation of NF-κB and MAPK/ERK 1/2 could be responsible for the accelerated development of atherosclerosis in RGS5-deficient mice.

CONCLUSIONS AND IMPLICATIONS

RGS5 deletion accelerated development of atherosclerosis and decreased the stability of atherosclerotic plaques partly through activating NF-κB and the MEK-ERK1/2 signalling pathways.

LINKED ARTICLES

This article is part of a themed section on Chinese Innovation in Cardiovascular Drug Discovery. To view the other articles in this section visit http://dx.doi.org/10.1111/bph.2015.172.issue-23

Abbreviations

ApoE, apolipoprotein E; CHD, coronary heart disease; H&E, haematoxylin-eosin; ICAM-1, intercellular adhesion molecue-1; LDL, low-density lipoprotein; MEK, MAPK/ERK kinase; RGS, regulator of G-protein signalling; SMC, smooth muscle cell; VCAM-1, vascular cell adhesion molecule-1

Tables of Links

TARGETS
Enzymes
Caspase 3
ERK1/2
JNK1/2
MEK 1
MEK 2
p38 (kinase)

LIGANDS
ICAM-1
IL-10
IL-1β
IL-6
RGS5
TNFα
VCAM-1

These Tables list key protein targets and ligands in this article which are hyperlinked to corresponding entries in http://www.guidetopharmacology.org, the common portal for data from the IUPHAR/BPS Guide to PHARMACOLOGY (Pawson *et al.*, 2014) and are permanently archived in the Concise Guide to PHARMACOLOGY 2013/14 (Alexander *et al.*, 2013).

Introduction

Atherosclerosis is a crucial pathophysiological condition underlying cardiovascular disease, the leading cause of mortality and morbidity in Western countries (Lloyd-Jones *et al.*, 2010). Over the last dozen years, compelling evidence has demonstrated that atherosclerosis is a chronic inflammatory disease (Ross, 1999; Libby, 2002) that is initiated by oxidative modification of low-density lipoprotein (LDL)-induced activation of endothelial dysfunction and that the subsequent secretion of chemokines and adhesion molecules attracts monocytes, which adhere to and migrate into the atherosclerotic lesions, where they differentiate into macrophages (Ley *et al.*, 2007). Recently, the recognition of this process of atherosclerosis, including the defining features of 'vulnerable plaques', has been receiving substantial attention as a risk factor for the occurrence of various acute cardiovascular events, such as myocardial infarction, sudden cardiac death and stroke (Virmani *et al.*, 2002). Thus, identifying the underlying molecular mechanisms that may attenuate atherosclerotic plaque progression and ultimate rupture is necessary for developing effective preventive and therapeutic strategies.

The regulator of G-protein signalling (RGS) proteins constitute a family of proteins that has been identified as providing negative regulation of G–protein-mediated receptor signalling pathways, which are required for many biological processes through the control of cellular function. These RGS proteins act as GTPase-activating proteins (GAPs) and stimulate the hydrolysis of the Gα-bound GTP back to GDP, resulting in the re-association of the Gβγ subunit (Hollinger and Hepler, 2002). As a member of the B/R4 family, expression of RGS5 is enriched in the aorta, heart and skeletal muscle, particularly in pericytes, smooth muscle cells (SMC), and endothelial cells of cardiovascular tissues (Adams *et al.*, 2000; Kirsch *et al.*, 2001; Cho *et al.*, 2003). To date, an increasing number of studies support the important role of RGS5 in endothelial function (Bondjers *et al.*, 2003; Furuya *et al.*, 2004; Hamzah *et al.*, 2008; Gu *et al.*, 2009). RGS5 has been identified as the first marker of angiogenic pericytes and is responsible for vessel remodelling, correlated with skin wound healing and tumour angiogenesis (Gu *et al.*, 2009). In the tumour vasculature of human renal cell carcinoma, RGS5 is highly expressed in endothelial cells (Furuya *et al.*, 2004). RGS5 deficiency results in pericyte maturation and vascular normalization and consequently improves the status of tumour hypoxia and reduces the leakiness of angiogenic vessels (Hamzah *et al.*, 2008). This effect is similar to the observation that after transient cerebral ischaemia, the loss of RGS5, especially in pericytes surrounding brain capillaries, ameliorates oedema by reducing vascular permeability (Bondjers *et al.*, 2003). Under the specific circumstance of hypoxia, RGS5 is reported to have an effect on the survival of endothelial cells (Jin *et al.*, 2009). Moreover, RGS5 deletion increases dyslipidaemia, obesity, adipose tissue deposition, hepatic steatosis and circulating inflammation (Deng *et al.*, 2012). However, little information is available on the function of RGS5 during the development of atherosclerosis.

In our study, a marked down-regulation of RGS5 expression was observed in atheromatous plaques, from patients and from a mouse model of atherosclerosis induced by lack of apolipoprotein E ($ApoE^{-/-}$ mice). We therefore hypothesized that changes in endothelial cell-derived RGS5 could be causally involved in atherogenesis. We used $ApoE^{-/-}$ mice also lacking RGS5 ($RGS5^{-/-}$;$ApoE^{-/-}$) to evaluate the regulatory effects of RGS5 on atherosclerosis and the potential underlying mechanisms.

Methods

Mice and diets

All animal care and experimental procedures were approved by the Animal Care and Use Committee of the Renmin Hos-

pital of Wuhan University and the Institutional Review Board for Human Studies of Nanjing Medical University. All studies involving animals are reported in accordance with the ARRIVE guidelines for reporting experiments involving animals (Kilkenny *et al.*, 2010; McGrath *et al.*, 2010). A total of 60 animals were used in the experiments described here.

The double-knockout mice were generated by crossing ApoE$^{-/-}$ mice with RGS5 deletion (Li *et al.*, 2010) and ApoE$^{-/-}$ littermates, 8 weeks of age, were used for the experiments. The 25 mice from each group were fed a high-fat diet (15.8% fat and 1.25% cholesterol of diet) for up to 28 weeks. Body weight and fasting glucose levels were measured at the beginning of the experiment and when they were killed.

En face *analysis of atherosclerosis and plaque histology*

For *en face* analysis of the atherosclerotic lesions, the entire aorta, including the subclavian and the right and left common carotid arteries, were removed and stained with Oil Red O; the lesion areas were quantified with Image Pro Plus 6.0 (Image Metrology, Copenhagen, Denmark). Hearts were fixed in 4% paraformaldehyde and embedded in paraffin or OCT for the histological procedures. Consecutive 5 μm sections of the atrioventricular valve region of the heart were collected and stained with haematoxylin–eosin (H&E) for morphology or with Picrosirius Red to evaluate collagen deposition. For the morphometric analysis, lesion size was measured on six consecutive sections in 100 μm intervals from 10 different littermates in each group using Image Pro Plus 6.0. The Plaque stability score = (SMC area + collagen area) / (macrophage area + lipid area).

Quantitative real-time PCR and Western blotting

Total mRNA was collected from the whole aorta using TRIzol reagent (Invitrogen, Carlsbad, CA, USA), and DNase-treated RNA was reverse transcribed with a transcriptor first strand cDNA Synthesis Kit (Roche, Indianapolis, IN, USA). The examined genes were confirmed by quantitative real-time PCR using LightCycler 480 SYBR Green 1 Master Mix (Roche) and the LightCycler 480 QPCR System (Roche); the relative transcript was normalized against GAPDH gene expression. Proteins were extracted from the aorta, which was homogenized in lysis buffer as described previously (Jiang *et al.*, 2014). Total protein and nuclear protein were extracted from the whole aorta and primary cells respectively. Five micrograms of protein was separated by SDS-PAGE (Invitrogen) and transferred to PVDF membranes (Millipore, Beijing, China). The membranes were blocked in Tris-buffered saline containing 5% non-fat milk for 1 h at room temperature and incubated with primary antibodies overnight at 4°C. Next, after incubation with secondary antibodies, the membranes were treated with ECL reagents (170–5061; Bio-Rad, Hercules, CA, USA) before being visualized using a FluorChem E Imager (Proteinsimple, San Jose, CA, USA). The specific protein expression was normalized against GAPDH protein expression. The following primary antibodies were used: RGS5 (Santa Cruz Biotechnology Inc., Dallas, TX, USA; L16), P-JNK1/2 (Cell Signaling Technology Inc., Danvers, MA, USA; 4668S), T-JNK1/2/3 (Bioworld; BS3630), P-MEK1/2 (Cell Signaling Technology Inc.; 9154), T-MEK1/2 (Cell Signaling Technology Inc.; 9122), P-ERK1/2 (Bioworld Technology Inc., St Louis Park, MN, USA; BS5016), T-ERK1/2 (Bioworld Technology Inc.; BS3627), P-p38 (Bioworld Technology Inc.; BS4766), T-p38 (Bioworld Technology Inc.; BS3566), Cleaved-caspase 3 (Cell Signaling Technology Inc.; 9661), p-IκBα (Cell Signaling Technology Technology Inc.; 9246), T-IκBα (Cell Signaling Technology Inc.; 4814), P-p65 (Bioworld Technology Inc.; BS4135) and T-p65 (Cell Signaling Technology Inc.; 4764S).

Immunofluorescence and TUNEL staining

The cross-section samples of the aortic sinus were used for immunofluorescence. After deparaffination or drying in a ventilation hood, the slides were blocked in 10% goat serum diluted with PBS for 1 h and incubated overnight with various primary antibodies: anti-RGS5 (goat polyclonal, 1:200 dilution, Santa Cruz Biotechnology), anti-CD31 (rabbit polyclonal, 1:50 dilution, Abcam, Cambridge, MA, USA; goat polyclonal, 1:50 dilution, Santa Cruz Biotechnology), anti-CD68 (rat monoclonal, 1:50 dilution, Bio-Rad), anti-smooth muscle actin (rat polyclonal, 1:100 dilution, Abcam), anti-phospho p65 (rabbit monoclonal, 1:50 dilution, Bioworld Technology Inc.), anti-ICAM-1 (goat polyclonal, 1:100 dilution, R&D Systems, Minneapolis, MN, USA), anti-vascular cell adhesion molecule-1 (VCAM-1; rat monoclonal, 1:100 dilution, Abcam), anti-phospho ERK (rabbit monoclonal, 1:200 dilution, Cell Signaling Technology Inc.), anti-IL-6 (goat polyclonal, 1:100 dilution, R&D Systems) and anti-IL-10 (goat polyclonal, 1:100 dilution, R&D Systems). After rewarming at 37°C for 1 h, the sections then were washed in PBS and incubated with the relevant secondary antibody for another 1 h. The secondary antibodies used were Alexa Fluor 488 and 568 donkey anti-rabbit IgG (1:200 dilution, Invitrogen), Alexa Fluor 568 donkey anti-goat IgG (1:200 dilution, Invitrogen), and Alexa Fluor 568 donkey anti-rat IgG (1:200 dilution, Invitrogen). The nuclei were stained with DAPI. For the co-staining of TUNEL and CD31, CD68 or cleaved-caspase3, the tissue sections were first stained with CD31, CD68 or cleaved-caspase3 antibody, followed by TUNEL staining with an ApopTagPlus In Situ Apoptosis Fluorescein Detection Kit (S7111, Millipore) according to the manufacturer's protocol. Images were obtained using a fluorescence microscope (OLYMPUS BX51, Shinjuku-ku, Tokyo, Japan) and the DP2-BSW software (version2.2, Shinjuku-ku, Tokyo, Japan) and the images were analysed with Image Pro Plus 6.0.

Human specimens

All of the procedures involving human samples complied with the principles outlined in the Declaration of Helsinki and were approved by the Renmin Hospital of Wuhan University Institutional Review Board in Wuhan, China. Written informed consent was obtained from relevant families. The relevant details of the patients are provided in Table 1. Samples of atheromatous plaques were collected from the coronary artery of coronary heart disease (CHD) patients, and the control samples were obtained from the coronary artery of normal heart donors, when the hearts were not suitable for transplantation, for non-cardiac reasons.

Data analysis

The given data are expressed as the mean ± SEM. The comparisons among the groups were evaluated using a two-tailed

Table 1
Relevant details of patients

Type	Gender	Age (years)	Medications (major)
CHD	Female	61	Nitroglycerin, dexamethasone, atorvastatin, heparin sodium
CHD	Male	42	Nicorandil, spirolactone, simvastatin, heparin sodium
CHD	Male	58	Atorvastatin, furosemide, trimetazidine, nicorandil
CHD	Male	63	Atorvastatin, metoprolol, heparin sodium
Donor	Male	56	N/A
Donor	Male	58	N/A
Donor	Male	36	N/A
Donor	Female	57	N/A

CHD, coronary heart disease; N/A, not available.

Student's *t*-test. All statistical analyses were performed with the Statistical Package for the Social Sciences (SPSS) software, version 16.0 (SPSS, Inc., Chicago, IL, USA). A P value < 0.05 was considered to be statistically significant.

Results

Down-regulation of RGS5 in atheromatous plaques from humans and ApoE-deficient male mice

To explore the potential role of RGS5 in the development of atherosclerosis, we examined whether RGS5 expression levels were altered in the endothelial cells of the atherosclerotic lesions. First, a morphological analysis based on H&E staining was performed using the right coronary artery from CHD patients, which is recognized as an atherosclerosis-prone region, to assess the lesion grade according to the definition and classification method (Stary *et al.*, 1995). Type V lesions showed several aspects of advanced atherosclerosis, such as fibrous thickening and cores of extracellular lipids (indicated by the black arrow), relative to the artery with no plaque from donated hearts from normal donors, which had not been used for transplantation because of non-cardiac reasons (Figure 1A). Next, double-immunofluorescence staining of the human coronary artery wall was performed to explore the expression of RGS5 and CD31 (a marker of endothelial cells). The representative images of obvious lesions (type V) revealed decreased expression of RGS5 in the endothelial cell layer compared with that in the non-atherosclerotic lesions (Figure 1C and E). Subsequently, to determine whether atherosclerotic lesions from the mouse model also showed decreased RGS5 expression in the endothelial cells, we grouped atherosclerosis-prone ApoE-deficient ($ApoE^{-/-}$) mice were treated with either normal chow or a high-fat Western diet for 28 weeks. The latter group exhibited large plaques in the case of hyperlipaemia, as shown in the representative H&E image (Figure 1B). As expected, similar results were obtained with immunofluorescence co-staining; Expression of RGS5 was markedly decreased in the endothelial cells of the atherosclerotic lesions induced by the high-fat diet (Figure 1D and E). Taken together, these data suggest that the down-regulation of RGS5 expression was concomitant with atherosclerosis-associated endothelial cell activation in both mouse and human atherosclerotic plaques.

RGS5 deficiency accelerates the development of atherosclerosis

Next, to investigate whether RGS5 deletion in atherosclerotic lesions contributes to accelerated atherosclerosis, $RGS5^{-/-}$ $ApoE^{-/-}$ mice were generated by crossing $RGS5^{-/-}$ strain with $ApoE^{-/-}$ mice and identified by Western blot (Figure 2A). Then we placed groups of male $RGS5^{-/-}ApoE^{-/-}$ and $ApoE^{-/-}$ littermates on a high-fat diet for almost 28 weeks, starting from 8 weeks of age. Although the high-fat diet led to hyperlipidaemia, there was no significant difference in the body weight or fasting glucose between the two genotypes (Table 2). *En face* analyses of the total aorta surface stained with Oil Red O revealed larger atherosclerotic lesions, and the quantitative data showed a 41% increase in $RGS5^{-/-}ApoE^{-/-}$ mice, compared with the $ApoE^{-/-}$ mice (Figure 2B). In addition, we further analysed advanced atherosclerotic lesions at the aortic root stained with H&E. Quantitative analysis of representative images exhibited enhanced lesion areas in cross-sections of the aortic sinus that were 30% larger in $RGS5^{-/-}ApoE^{-/-}$ mice than in $ApoE^{-/-}$ controls (Figure 2C). We also analysed the necrotic cores of the plaques, a major determinant of plaque vulnerability. These cores initially result from the accumulation of apoptotic macrophages because of defective efferocytosis (Tabas, 2010). Analysis of lesions with thickened fibrous caps (indicated by the black arrows) revealed a pronounced increase in the total necrotic area, which was quantified at 38%, in the lesions of $RGS5^{-/-}ApoE^{-/-}$ (Figure 2D). Collectively, these results together with the increased lesion and necrotic areas in $RGS5^{-/-}ApoE^{-/-}$ mice demonstrate that RGS5 deficiency accelerated the development of atherosclerosis in this model.

RGS5 deficiency increases expression of inflammatory mediators

To examine whether enhanced inflammation is responsible for the severity of atherosclerotic lesions *in vivo*, we assessed the expression of inflammatory mediators, including cytokines and adhesion molecules, which contribute to the

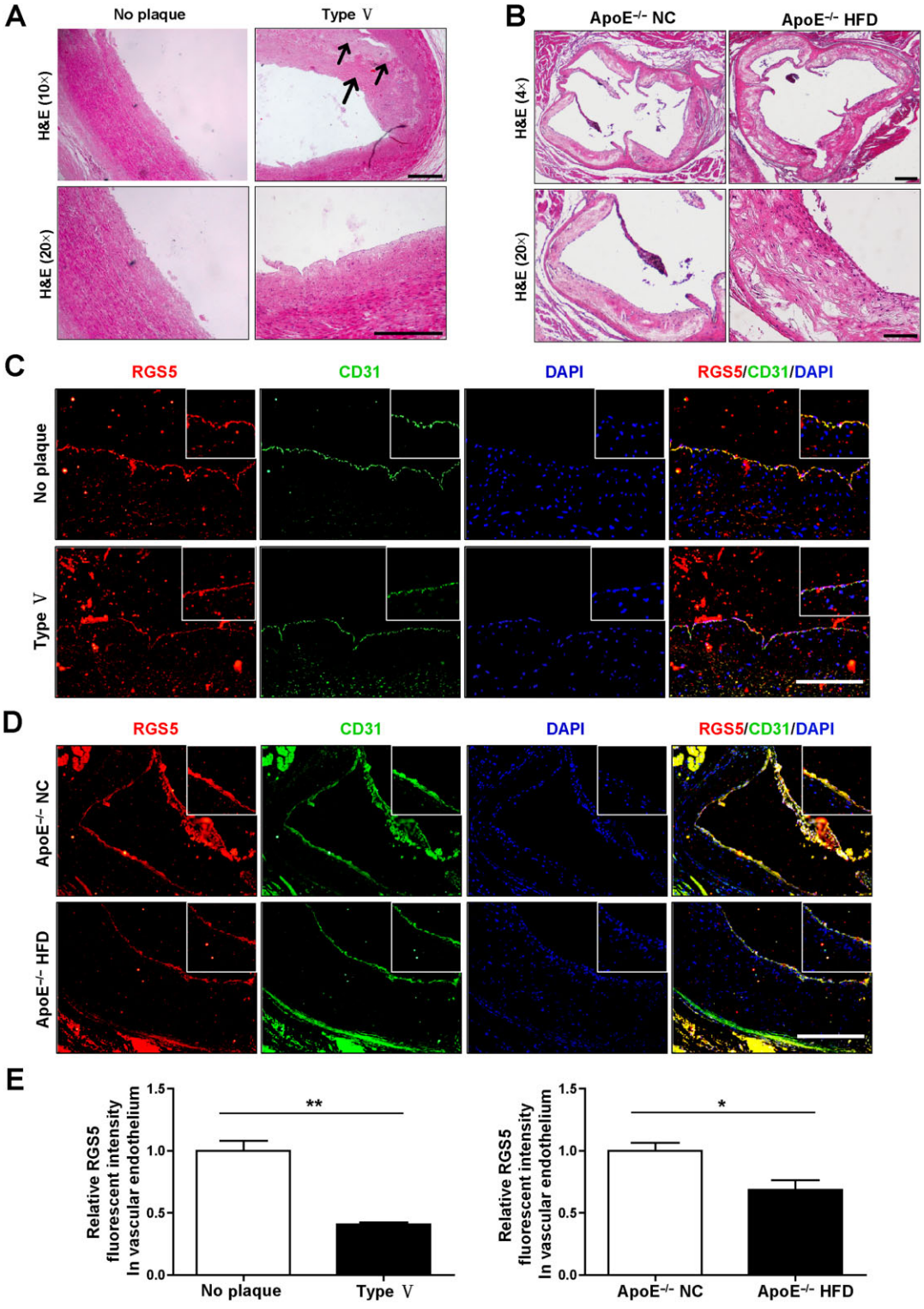

Figure 1

Decreased expression of RGS5 in atheromatous plaques of human coronary artery and ApoE$^{-/-}$ mice. (A) Serial sections of human coronary artery from patients with CHD were stained with H&E and scored via the Stary classification method . The arrow indicates cap thickness and cores of extracellular lipid. Representative images are shown (original magnification, ×10 and ×20). Scale bar = 200 μm. (B) Cross-sections of the aortic sinus from ApoE$^{-/-}$ mice fed either normal chow or a high-fat diet and stained with H&E. Representative images are shown (original magnification, ×4 and ×20). Scale bar = 200 μm. (C, D) Representative images showing double-immunofluorescence staining of human coronary arteries or cross-sections of the aortic sinus from ApoE$^{-/-}$mice, for RGS5 (red) and CD31 (endothelium, green). Scale bar = 200 μm. (E) Quantification of RGS5 fluorescent intensity in vascular endothelium of human and mice tissues. $^{**}P < 0.01$, $^{*}P < 0.05$ compared with ApoE$^{-/-}$.

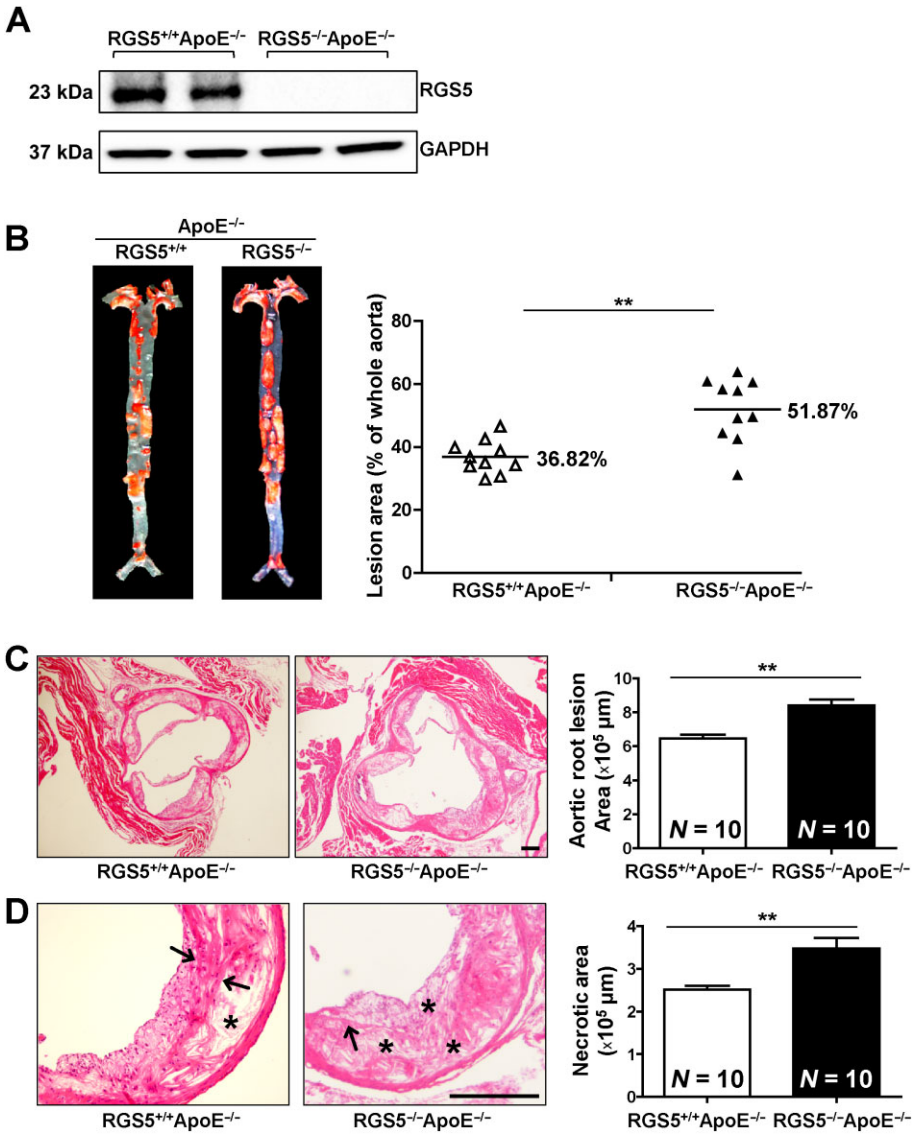

Figure 2

Deficiency of RGS5 promotes atherosclerosis in ApoE$^{-/-}$mice. (A) The expression of RGS5 in RGS5$^{-/-}$ApoE$^{-/-}$ mice and ApoE$^{-/-}$ controls. (B) Representative images of *en face* Oil Red O staining of aortas of RGS5$^{-/-}$ApoE$^{-/-}$ and ApoE$^{-/-}$ littermates, $n = 10$. $^{**}P < 0.01$ compared with ApoE$^{-/-}$. (C) (left panel) Representative images of cross-sections of the aortic sinus stained with H&E. (right panel) Quantification of the atheroma area. Six slides from different layers from at least 10 hearts in each group were used for the analysis. Scale bar = 200 μm; $n = 10$. $^{**}P < 0.01$ compared with ApoE$^{-/-}$. (D) (Left panel) Representative sections of H&E-stained aortic root sections from RGS5$^{-/-}$ApoE$^{-/-}$ and ApoE$^{-/-}$ mice; * = necrotic areas). The area between the arrows indicates cap thickness. (right panel) Quantification of anuclear, afibrotic, and eosin-negative necrotic areas. Scale bar = 200 μm; $n = 10$.$^{**}P < 0.01$ compared with ApoE$^{-/-}$.

formation of atherosclerotic lesions. Analysis of the expression of adhesion molecules ICAM-1 and VCAM-1 by RT-PCR showed a robust increase in the RGS5$^{-/-}$ApoE$^{-/-}$ mice relative to the ApoE$^{-/-}$ controls (Figure 3A). Immunostaining of the aortic root cross-sections with ICAM–1-specific antibodies revealed a similar increased expression of ICAM-1 in the endothelial cell layer of RGS5$^{-/-}$ApoE$^{-/-}$ mice compared with ApoE$^{-/-}$ littermates (Figure 3B). Similar approaches were used to analyse the expression of VCAM-1 in the endothelial cells of the atherosclerotic lesions. Compared with ApoE$^{-/-}$mice, a moderate increase of VCAM-1 expression in the endothelial cell layer was observed in RGS5$^{-/-}$ApoE$^{-/-}$ mice, whereas this increase was much more significant in the lesion areas of RGS5$^{-/-}$ApoE$^{-/-}$ mice (Figure 3C). Additionally, the mRNA levels of pro-inflammatory markers, IL-6, IL-1β and TNF-α were increased in the atherosclerotic lesions of RGS5$^{-/-}$ApoE$^{-/-}$ mice compared with ApoE$^{-/-}$ mice, whereas the anti-inflammatory IL-10 showed the opposite result (Figure 3A). Further, immunofluorescence staining analysis of IL-6 and IL-10 in the lesions from RGS5$^{-/-}$ApoE$^{-/-}$ mice exhibited results consistent with their mRNA level (Figure 3D). Given that NF-κB plays a pivotal role in the inflammation that

Table 2

Metabolic characteristics of RGS5$^{-/-}$ApoE$^{-/-}$mice and ApoE$^{-/-}$mice after 28 week feeding with high-fat diet

Mice	Index	0 week high-fat diet	28 week high-fat diet
ApoE$^{-/-}$ (N = 25)	Body weight, g	24.0 ± 1.7	35.6 ± 8.1
	Glucose, mg·L^{-1}	79 ± 9	86 ± 10
RGS5$^{-/-}$ApoE$^{-/-}$ (N = 25)	Body weight, g	24.6 ± 2.3	38.6 ± 10.1
	Glucose, mg·L^{-1}	79 ± 10	89 ± 6

No significant difference was found between two groups of mice fed for 28 weeks.

contributes to the pathogenesis of atherosclerosis, the expression of NF-κB P65 subunit was further measured. As shown in Figure 3D, consistent with the presence of these elevated inflammatory mediators, increased nuclear translocation of the P65 was observed in lesions from RGS5$^{-/-}$ApoE$^{-/-}$ mice, compared with that in ApoE$^{-/-}$ controls.

RGS5 deletion promotes apoptosis of endothelial cells and macrophages

Apoptosis of endothelial cells facilitates the extravasation of monocytes and leads to the development of atherosclerosis. As shown in the representative images and the quantitative data, the number of TUNEL-positive endothelial cells was increased (by 70%) in RGS5$^{-/-}$ApoE$^{-/-}$ mice, compared with ApoE$^{-/-}$ littermates (Figure 4A). Macrophage apoptosis plays an important role in atherosclerotic plaque development (Tabas, 2010). We observed an increase in the percentage of TUNEL, and CD68-positive macrophages in atherosclerotic lesions in RGS5$^{-/-}$ApoE$^{-/-}$ mice compared with ApoE$^{-/-}$ mice (Figure 4B). Meanwhile, immunofluorescent co-staining with cleaved-caspase 3 and TUNEL, displayed an increase in the percentage of caspase 3/TUNEL-positive cells in the atherosclerotic plaque of RGS5$^{-/-}$ApoE$^{-/-}$ mice, compared with that in ApoE$^{-/-}$ mice (Figure 4C).

Enhanced instability of atherosclerotic plaques in the absence of RGS5

To further explore the effects of RGS5 deficiency on the stability of atherosclerotic plaques, other properties of plaque composition contributing to plaque instability were investigated, including decreased collagen content and SMC content covering the fibrous cap, increased macrophage numbers and increased lipid accumulation. First, the percentage of collagen in RGS5$^{-/-}$ApoE$^{-/-}$ mice showed a 37% reduction relative to the ApoE$^{-/-}$ littermates (Figure 5A and E). Second, the SMC content of the atherosclerotic lesions showed a coordinated effect with a significant decrease of 48% in RGS5$^{-/-}$ApoE$^{-/-}$ mice, compared with the controls (Figure 5B and E). Third, the macrophage infiltration that contributes to the formation of foam cells critical for atherogenesis was increased by 28% within lesions from RGS5$^{-/-}$ApoE$^{-/-}$ mice, compared with the ApoE$^{-/-}$ mice (Figure 5C and E). Finally, lipid area staining with Oil Red O revealed a robust 39% increase in lipid accumulation in the lesions from RGS5$^{-/-}$ApoE$^{-/-}$ mice, compared with ApoE$^{-/-}$ controls. Furthermore, we scored plaque stability, as described earlier, and the results showed an almost 50% decrease in RGS5$^{-/-}$ApoE$^{-/-}$ mice (Figure 5F). This evidence indicates that RGS5 plays a protective role in advanced atherosclerotic lesions by enhancing several aspects of atherosclerotic plaque stability at the aortic root.

Loss of RGS5 activated the NF-κB and MEK-ERK1/2 signalling pathways

To identify the potential molecular mechanisms through which RGS5 slowed the development of atherosclerosis, we examined the state of activation of the NF-κB and MEK-ERK1/2 signalling pathways. Markedly increased expression of phosphorylated ERK1/2 was observed by co-staining with CD31 in RGS5$^{-/-}$ApoE$^{-/-}$ mice, compared with ApoE$^{-/-}$ controls (Figure 6A). Further analysis of the phosphorylated levels of MEK1/2, ERK1/2, P38, JNK1/2, and p65 was carried out by Western blotting. Although levels of p65 and MEK-ERK1/2 phosphorylation were increased in RGS5$^{-/-}$ApoE$^{-/-}$ mice, there was no statistically significant difference in p38 and JNK1/2 between the two groups (Figure 6B). To further confirm the involvement of these molecular changes, peritoneal macrophages were isolated from RGS5$^{-/-}$ApoE$^{-/-}$ mice; these cells showed no detectable levels of RGS5 by Western blot (Figure 6C). Peritoneal macrophages were similarly isolated from ApoE$^{-/-}$ littermates. The expression of phosphorylated ERK1/2, and NF-kB, as well as markers of apoptosis were measured after treatment of both sets of macrophages with oxidized LDL for 24 h. There was a marked increase in the levels of phosphorylated ERK1/2, phospho-p65, IκBα, and cleaved-caspase 3 in the macrophages from RGS5$^{-/-}$ApoE$^{-/-}$ mice, compared with those from ApoE$^{-/-}$ controls (Figure 6C). These results suggest that RGS5 inhibited atherosclerosis, at least partly, by inhibiting MEK-ERK1/2 and NF-κB signalling.

Discussion

In the present study, we assessed a novel role for RGS5 in endothelial cells from atherosclerotic lesions. RGS5 deficiency not only accelerated development of atherosclerosis, but also decreased the stability of atherosclerotic plaques. A mechanistic analysis suggested that this effect of RGS5 on atherosclerosis could derive, in part, from its regulatory effects on NF-κB and MEK-ERK1/2 signalling pathways.

Endothelial dysfunction, including enhanced permeability and pro-inflammatory changes, is associated with endothelial cell apoptosis and deteriorating endothelial function to induce vascular pathogenesis and is recognized as

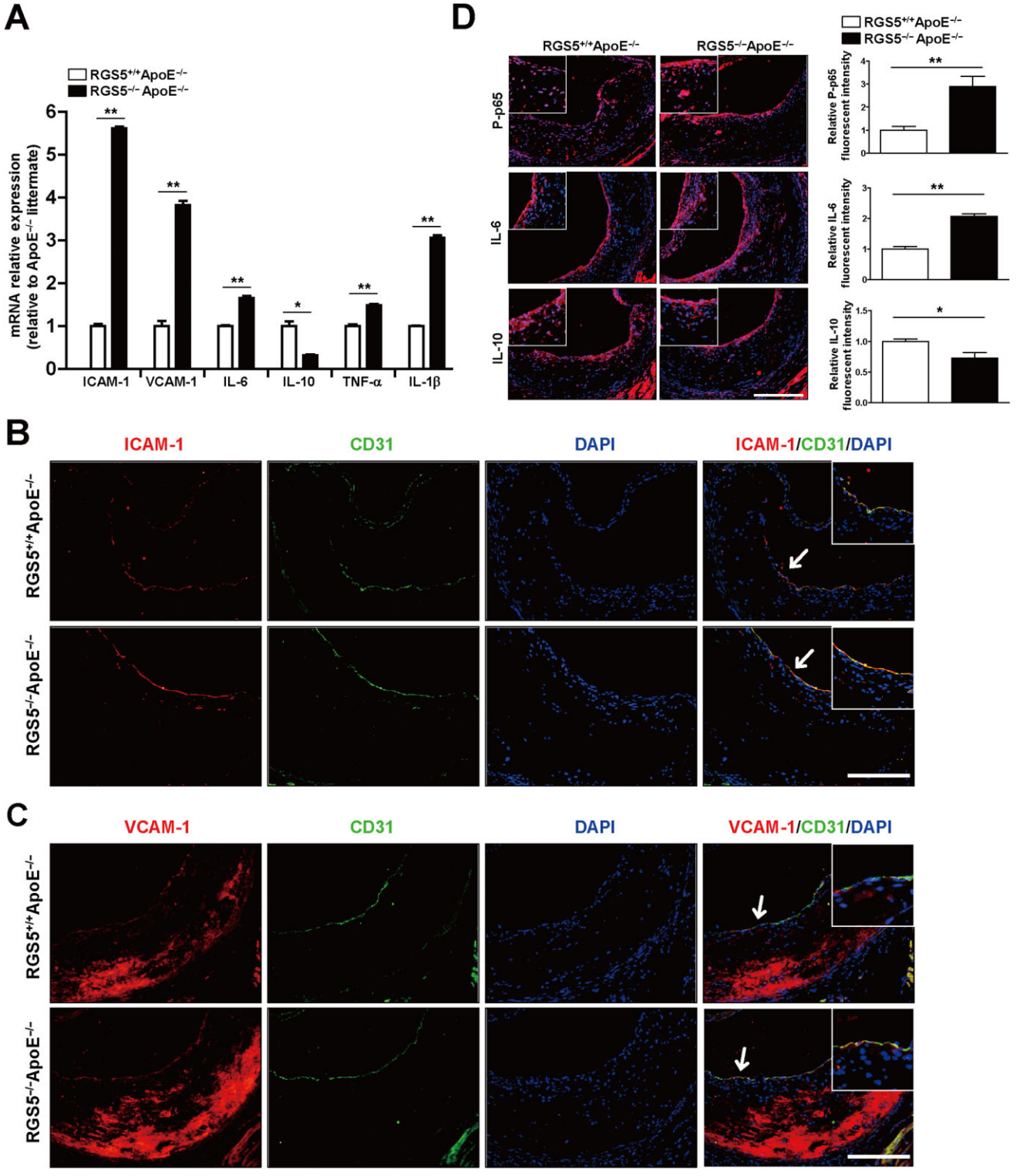

Figure 3

Deletion of RGS5 enhances the expression of adhesion molecules and the inflammatory response. (A) Real-time PCR assays were performed to determine the RNA levels of two adhesion molecules, ICAM-1 and VCAM-1, and several general inflammatory mediators. The expression of these transcripts was quantified as relative mRNA expression after normalization to GAPDH expression. $^{**}P < 0.01$,$^{*}P < 0.05$ compared with ApoE$^{-/-}$. (B, C) Immunofluorescent co-staining of atherosclerotic plaques with ICAM-1 (red) or VCAM-1 (red) and CD31 (endothelium, green). Representative images are shown (×20 magnification). Scale bar = 200 μm. (D) (Left panel) Representative images showing immunofluorescence staining of cross-sections of the aortic sinus for P-p65, IL-6 and IL-10. (right panel) Quantification of relative fluorescence intensity. Scale bar = 200 μm. $^{**}P < 0.01$,$^{*}P < 0.05$ compared with ApoE$^{-/-}$.

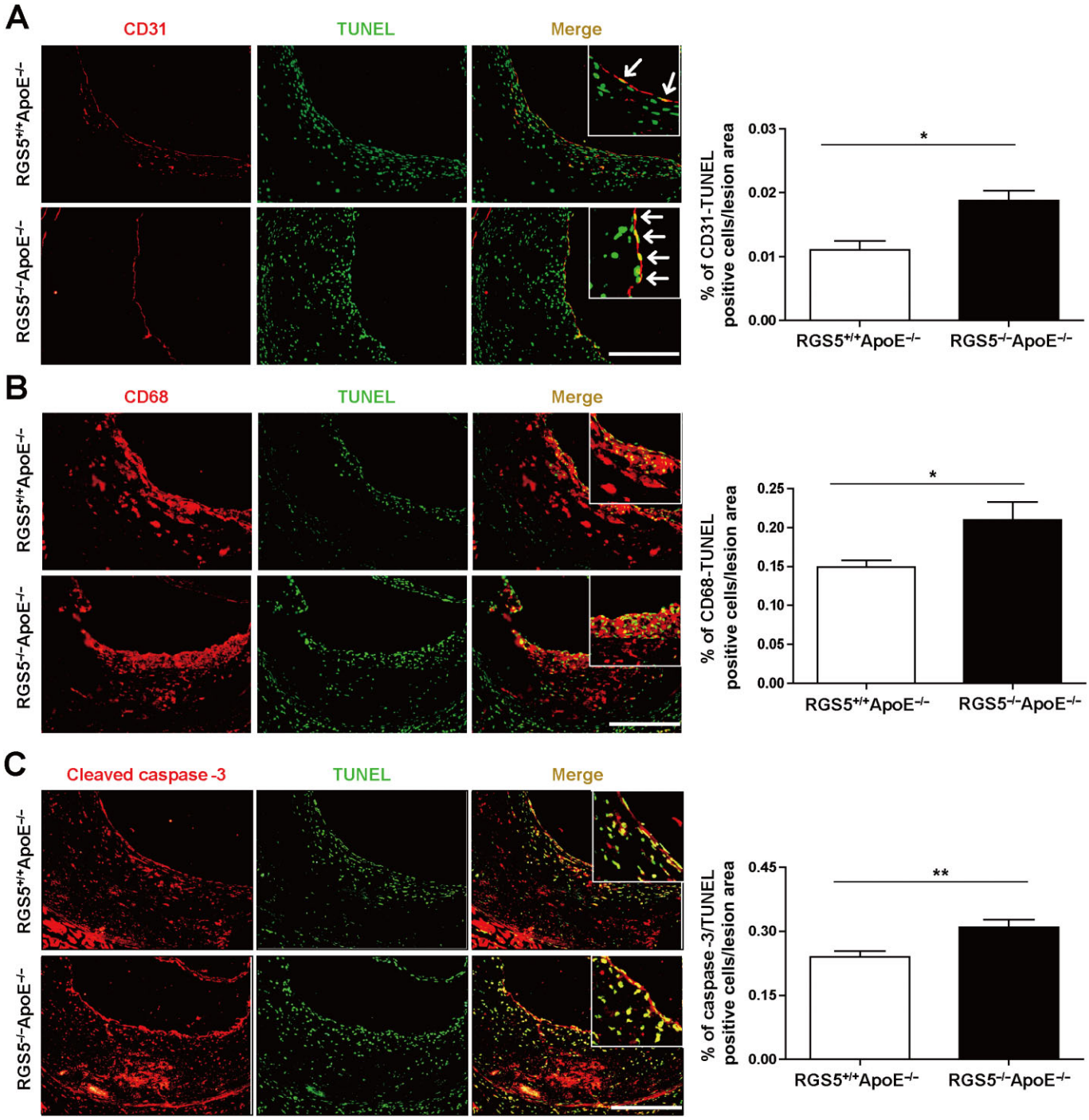

Figure 4

Increased apoptosis of endothelial cells and macrophages in the absence of RGS5. Apoptotic cells in the lesion area were detected by TUNEL staining, endothelial cells (A) by CD31 staining, and macrophages (B) by CD68 staining. Representative images are shown (X20 magnification) and quantitative data are shown to the right. Scale bar = 200 μm. *$P < 0.05$ compared with ApoE$^{-/-}$ (C) Immunofluorescent costaining with cleaved-caspase 3 (red) and TUNEL (green) of the aortic sinus. Scale bar = 200 μm. **$P < 0.01$ compared with ApoE$^{-/-}$.

the key outcome in the early inflammatory response to the oxidative modification of LDLs in the process of atherosclerosis (Harrison, 1997; Glass and Witztum, 2011). Here, we first demonstrated that RGS5 was down-regulated in the endothelial cell layer of atheromatous plaques, and that it promoted the apoptosis of endothelial cells. Analysis of the aortic root showed that ICAM-1 and VCAM-1 were dramatically up-regulated and abundantly expressed in different locations in the advanced stages of the disease process in RGS5$^{-/-}$ApoE$^{-/-}$ mice, as suggested by a previous study (Iiyama

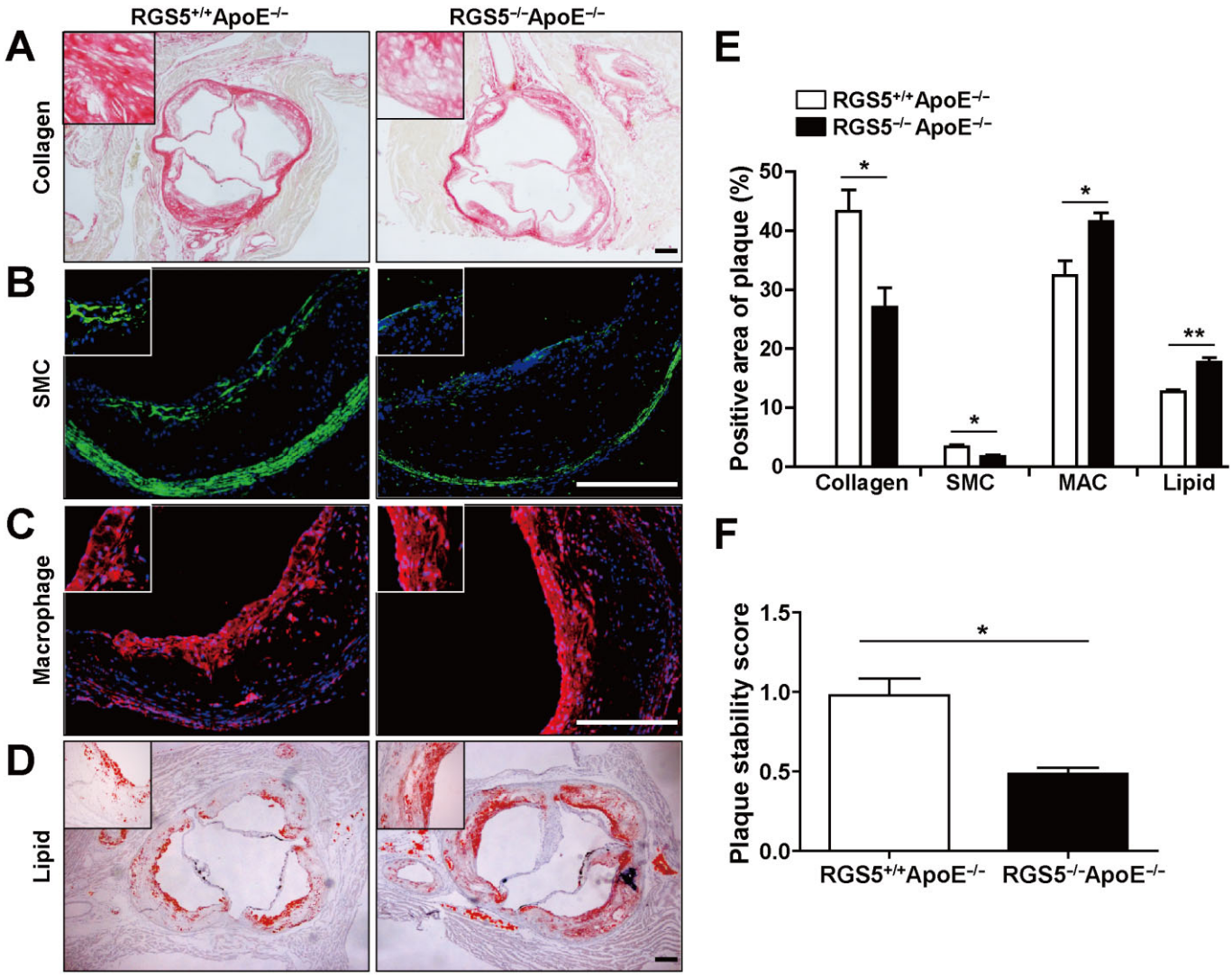

Figure 5

Plaques from RGS5$^{-/-}$ApoE$^{-/-}$ mice were less stable. Cross-sections of the aortic sinus plaques were stained with Picrosirius Red for collagen (A), smooth muscle actin for SMCs (B), CD68 for macrophages (C), and Oil Red O for lipid (D). Scale bar = 200 μm. (E) Plaques from RGS5$^{-/-}$ApoE$^{-/-}$ mice exhibited decreased percentages of collagen and SMCs and increased percentages of macrophages (MAC) and increased lipid area compared with those from ApoE$^{-/-}$ mice. $^{**}P < 0.01$,$^{*}P < 0.05$ compared with ApoE$^{-/-}$. (F) The plaque stability score of RGS5$^{-/-}$ApoE$^{-/-}$ mice was 70% lower than that of ApoE$^{-/-}$ mice. $^{*}P < 0.05$ compared with ApoE$^{-/-}$.

et al., 1999). Therefore, a possible explanation for the accelerated plaque development in RGS5$^{-/-}$ mice may be an intrinsic activation of endothelial cells. As already known, concomitant with increased proinflammatory cell adhesion molecules, VCAM-1 and ICAM-1, which were secreted by the activation of endothelial cells, the infiltration of macrophages originating from monocytes is markedly increased and plays a causal role in the severity of atherogenesis (Ley *et al.*, 2007; Mestas and Ley, 2008; Glass and Witztum, 2011). In our study, apart from the increased numbers of infiltrating macrophages, we also detected enhanced pro-inflammatory gene expression (IL-6, TNFα and IL-1β), which can be expressed in macrophages along with highly activated NF-κB signalling (Brand *et al.*, 1996). The results we obtained are consistent with a previous study that showed that endothelial cell-specific inhibition of NF-κB protected mice from atherosclerosis through various mechanisms, including reduced expression of proinflammatory cytokines, chemokines and adhesion molecules, and by interfering with the recruitment of monocytes into atherosclerotic plaques (Gareus *et al.*, 2008). During the past decade, activation of NF-κB has been identified in SMCs, macrophages and the endothelial cells of atherosclerotic lesions, and this activation played a crucial role in the regulation of inflammatory mediator expression (De Martin *et al.*, 2000). Against this background, our results would suggest that RGS5 deficiency in endothelial cells determines the severity of atherosclerosis, by increasing inflammation through activation of the NF-κB signalling pathway. Further research is required to determine whether RGS5 has a similar effect on the inflammatory responses in macrophages.

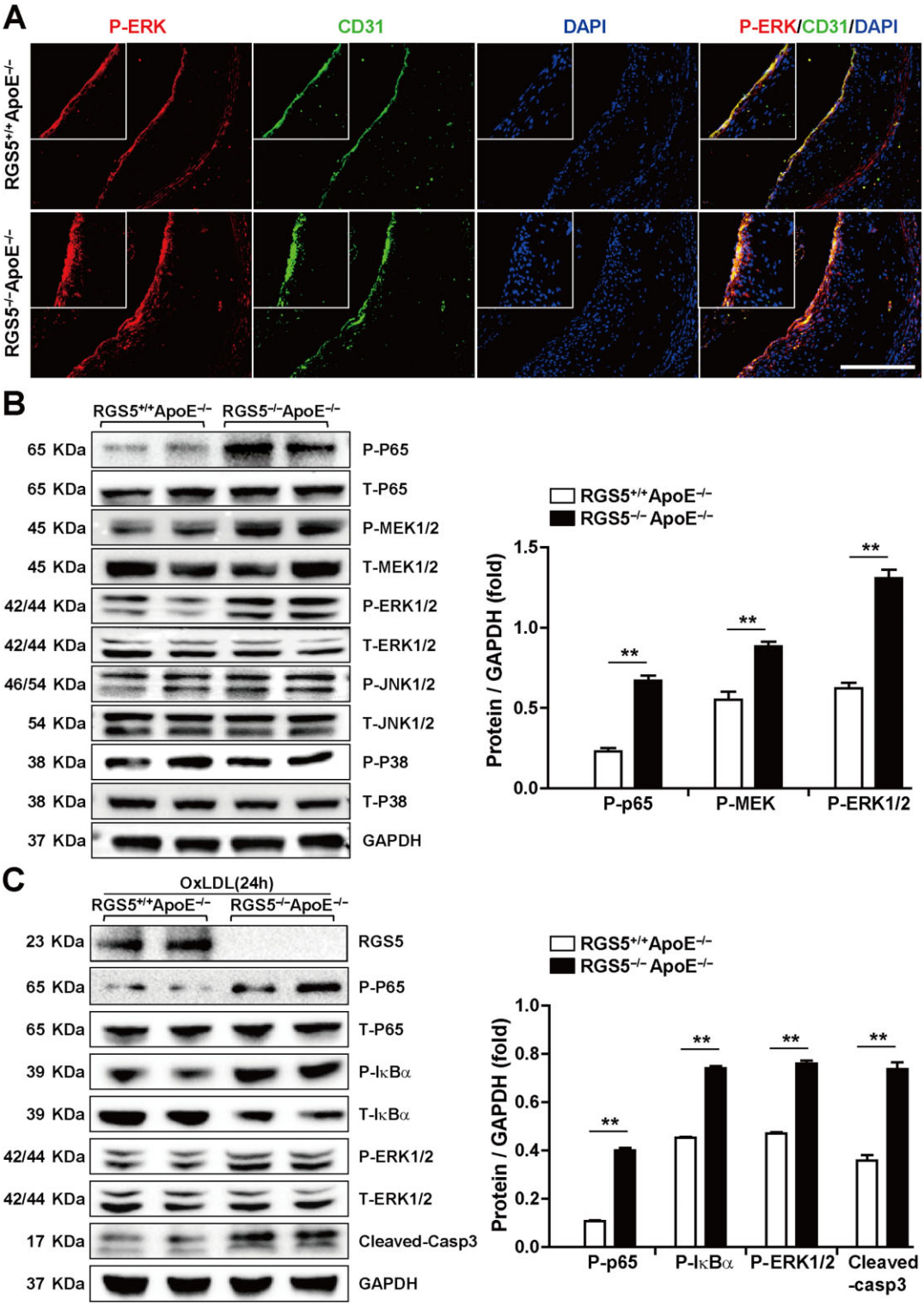

Figure 6

Effect of RGS5 on the MEK-ERK1/2 and NF-κB signalling pathways. (A) Immunofluorescent co-staining of atherosclerotic plaque with phosphorylated ERK1/2 (red) and CD31 (endothelium, green). Representative images are shown (×20 magnification). Scale bar = 200 μm. (B) Representative p65, MEK, ERK1/2, p38, and JNK phosphorylation and their total protein expression in RGS5$^{-/-}$ApoE$^{-/-}$ mice and ApoE$^{-/-}$ controls. The expression of these proteins was quantified as relative expression after normalization to GAPDH expression. **$P < 0.01$ compared with ApoE$^{-/-}$. (C) Representative RGS5, p65, IκBα, ERK1/2 phosphorylation, and cleaved-caspase 3 and their total protein expression in peritoneal macrophages from RGS5$^{-/-}$ApoE$^{-/-}$ mice and ApoE$^{-/-}$ littermates. The expression of these proteins was quantified as relative expression after normalization to GAPDH expression. **$P < 0.01$ compared with ApoE$^{-/-}$.

Interestingly, we also observed markedly decreased expression of IL-10. Thre is considerable circumstantial evidence for the anti-inflammatory properties of IL-10 in atherosclerosis *in vivo*. For example, the electrotransfer of IL-10 cDNA significantly decreased endothelial NF-κB activation and the expression of VCAM-1 and ICAM-1 (Potteaux *et al.*, 2006), and IL-10 deletion aggravated atherosclerosis (Mallat *et al.*, 1999). Therefore, our observation of decreased expression of IL-10 could, at least in part, contribute to the development of atherosclerosis.

Enhanced vessel wall permeability results from the apoptosis of vascular endothelial cells and facilitates the infiltration of cytokines, growth factors, lipids and immune cells, which increase the pro-coagulatory activity of endothelial cells and induce rupture of atherosclerotic plaques (Choy *et al.*, 2001). We found that apoptosis of macrophages and endothelial cells was increased in RGS5$^{-/-}$ApoE$^{-/-}$ mice. However, the relationship between macrophage apoptosis and atherogenesis is complex and requires further investigation (Tabas, 2005). Based on the examination and quantification of the lesions from the cross-section of the aortic sinus stained with H&E, we noticed that the total necrotic areas covered with fibrotic caps were almost 1.6-fold larger in RGS5$^{-/-}$ApoE$^{-/-}$ mice, relative to ApoE$^{-/-}$ controls. A previous study has documented that necrotic cores arise from apoptotic macrophages in advanced atherosclerotic lesions, where accumulation is more abundant than in early atherosclerotic lesions because of defective phagocytic clearance (Tabas, 2010). In human atherosclerotic-induced cardiovascular disease, plaque morphology is a more important predictor of plaque disruption and acute clinical events than plaque size and the size of the necrotic core, in particular, plays a major determining role in plaque vulnerability (Brown *et al.*, 1993). Other features, such as thinning of the fibrous cap, a high level of inflammatory cytokines, significant accumulation of lipids and apoptosis of intimal cells, also contribute to the vulnerability of atherosclerotic plaques (Kolodgie *et al.*, 2004; Clarke and Bennett, 2006). In our model, we demonstrated that RGS5 deficiency induced apoptosis in macrophages and increased inflammatory gene expression. Further analysis of the atherosclerotic plaques, in RGS5$^{-/-}$ApoE$^{-/-}$ mice, showed remarkably increased infiltration of macrophages accompanied by an accumulation of lipids and a decrease in the percentage of SMC and collagen. Advanced necrotic cores and other features of deterioration in vulnerable plaques are responsible for acute atherothrombotic clinical events. However, the mouse is not a good model for plaque disruption and acute atherothrombosis (Rosenfeld *et al.*, 2002; Virmani *et al.*, 2002). Nevertheless, our results still demonstrate a possible treatment option of targeting RGS5 in atherogenesis, particularly for maintaining plaque stability.

Although the present study has provided considerable evidence that RGS5 plays an important functional role in atherosclerosis, the mechanism by which RGS5 mediated its anti-atherosclerosis effects remains unclear. In an earlier study, RGS5 deletion increased dyslipidaemia, obesity, adipose tissue deposition, hepatic steatosis and circulating inflammation through JNK and NF-kB signalling pathways (Deng *et al.*, 2012). However, in our study, we found there were no significant differences in the levels of body weight, glucose, triglycerides, total cholesterol, high-density lipoprotein and LDL between the two groups of mice.

RGS5 also protected against cardiac hypertrophy and fibrosis by inhibiting MEK-ERK1/2 signalling (Li *et al.*, 2010) and MAPK signalling pathways play a key role in the progress of cardiac hypertrophy (Molkentin, 2004; Lu *et al.*, 2013; Li *et al.*, 2014). Additionally, the majority of the many MAPK pathways expressed in mammals, along with the NF-κB pathway, respond to inflammatory stimuli and a wide variety of other stimuli, including growth factors, GPCRs and environmental stresses such as oxidative stress and endoplasmic reticulum stress (Kyriakis and Avruch, 2001; 2012). The MAPK family consists of three major cascades, ERK, p38 and JNK. The JNK and p38 signalling pathways are activated by proinflammatory cytokines such as TNF-α and by IL-1β stimulation of endothelial cells or in response to cellular stresses such as genotoxic, osmotic, hypoxic or oxidative stress (Surapisitchat *et al.*, 2001). By contrast, ERKs can be activated in a manner independent of Ras by proinflammatory stimuli, including cytokines of the TNF family and endogenously produced danger signals such as oxidised LDL in atherosclerosis and crystalline uric acid in gout (Kyriakis and Avruch, 2012). Increased ERK1/2 phosphorylation in HUVECs and atherosclerotic plaques was a consequence of silencing RGS5 expression (Anger *et al.*, 2008). Therefore, we examined the status of the MAPK signalling pathway in the absence of RGS5 expression in our atherosclerosis models. First, *in vivo*, we found increased activation of phosphorylated MEK and ERK1/2 protein expression in RGS5$^{-/-}$ApoE$^{-/-}$ mice, whereas the phosphorylation of p38 and JNK1/2 was not affected. Consistent with these results, levels of phosphorylated ERK1/2, P-p65and P-IκBα, as well as the apoptotic marker, cleaved-caspase 3 were increased *in vitro*. Furthermore, phosphorylated ERK co-staining with CD31 was predominant in the endothelial cell layer of both groups and was more abundant in RGS5$^{-/-}$ApoE$^{-/-}$ mice, whereas there was minimal co-expression in the lesion area. Overall, the NF-κB and MEK-ERK1/2 signalling pathways appear to be critical components of the response to RGS5 deletion in atherosclerosis.

In conclusion, we have shown that RGS5 deletion, associated with endothelial cells, accelerated high-fat diet-induced atherogenesis and plaque instability by contributing to endothelial dysfunction and enhanced vascular inflammation through the activation of the NF-κB and MEK-ERK1/2 signalling pathways. Given that acute clinical cardiovascular events occur at sites of atherosclerosis because the rupture of atherosclerotic plaques is not prevented, our work highlights the important role of RGS5 as a pharmacological therapeutic target in this clinical situation. Further clinical investigation is needed to determine whether increased RGS5 levels constitute an effective treatment for underlying atherosclerosis in patients with CHD or whether RGS5 is a potential target for the prevention of atherogenesis and the stabilization of atherosclerotic plaques.

Acknowledgements

This work was supported by grants from the National Natural Science Foundation of China (Nos. 81100230, 81070089,

81200071, 81270306 and 81370365), National Science and Technology Support Project (Nos. 2011BAI15B02, 2012BAI39B05 and 2013YQ030923-05), the National Basic Research Program of China (Nos. 2011CB503902 and 2011CB503903), the Key Project of the National Natural Science Foundation (Nos. 81330005, 81330004), the Collaborative Innovation Center for Cardiovascular Disease Translational Medicine and the PAPD.

Author contributions

W.-L. C. and P.-X. W. designed and conducted *in vivo* experiments, analysed the data and drafted the paper. T. W. and C. D performed the establishment of animal model and the collection of experimental tissues. W.-L. C. and Y. Z. performed the pathological study and analysed the data. Y. J. and H. L. designed all of the experiments, supervised and funded the study, and contributed to the data analysis and to the writing of the paper.

Conflict of interest

None.

References

Adams LD, Geary RL, McManus B, Schwartz SM (2000). A comparison of aorta and vena cava medial message expression by cDNA array analysis identifies a set of 68 consistently differentially expressed genes, all in aortic media. Circ Res 87: 623–631.

Alexander SPH, Benson HE, Faccenda E, Pawson AJ, Sharman JL Spedding M *et al* (2013). The Concise Guide to PHARMACOLOGY 2013/14: Enzymes. Br J Pharmacol, 170: 1797–1867.

Anger T, Grebe N, Osinski D, Stelzer N, Carson W, Daniel WG *et al*. (2008). Role of endogenous RGS proteins on endothelial ERK 1/2 activation. Exp Mol Pathol 85: 165–173.

Bondjers C, Kalen M, Hellstrom M, Scheidl SJ, Abramsson A, Renner O *et al*. (2003). Transcription profiling of platelet-derived growth factor-B-deficient mouse embryos identifies RGS5 as a novel marker for pericytes and vascular smooth muscle cells. Am J Pathol 162: 721–729.

Brand K, Page S, Rogler G, Bartsch A, Brandl R, Knuechel R *et al*. (1996). Activated transcription factor nuclear factor-kappa B is present in the atherosclerotic lesion. J Clin Invest 97: 1715–1722.

Brown BG, Zhao XQ, Sacco DE, Albers JJ (1993). Atherosclerosis regression, plaque disruption, and cardiovascular events: a rationale for lipid lowering in coronary artery disease. Annu Rev Med 44: 365–376.

Cho H, Kozasa T, Bondjers C, Betsholtz C, Kehrl JH (2003). Pericyte-specific expression of Rgs5: implications for PDGF and EDG receptor signaling during vascular maturation. FASEB J 17: 440–442.

Choy JC, Granville DJ, Hunt DW, McManus BM (2001). Endothelial cell apoptosis: biochemical characteristics and potential implications for atherosclerosis. J Mol Cell Cardiol 33: 1673–1690.

Clarke M, Bennett M (2006). The emerging role of vascular smooth muscle cell apoptosis in atherosclerosis and plaque stability. Am J Nephrol 26: 531–535.

De Martin R, Hoeth M, Hofer-Warbinek R, Schmid JA (2000). The transcription factor NF-kappa B and the regulation of vascular cell function. Arterioscler Thromb Vasc Biol 20: E83–E88.

Deng W, Wang X, Xiao J, Chen K, Zhou H, Shen D *et al*. (2012). Loss of regulator of G protein signaling 5 exacerbates obesity, hepatic steatosis, inflammation and insulin resistance. PLoS ONE 7: e30256.

Furuya M, Nishiyama M, Kimura S, Suyama T, Naya Y, Ito H *et al*. (2004). Expression of regulator of G protein signalling protein 5 (RGS5) in the tumour vasculature of human renal cell carcinoma. J Pathol 203: 551–558.

Gareus R, Kotsaki E, Xanthoulea S, van der Made I, Gijbels MJ, Kardakaris R *et al*. (2008). Endothelial cell-specific NF-kappaB inhibition protects mice from atherosclerosis. Cell Metab 8: 372–383.

Glass CK, Witztum JL (2001). Atherosclerosis. The road ahead. Cell 104: 503–516.

Gu S, Cifelli C, Wang S, Heximer SP (2009). RGS proteins: identifying new GAPs in the understanding of blood pressure regulation and cardiovascular function. Clin Sci (Lond) 116: 391–399.

Hamzah J, Jugold M, Kiessling F, Rigby P, Manzur M, Marti HH *et al*. (2008). Vascular normalization in Rgs5-deficient tumours promotes immune destruction. Nature 453: 410–414.

Harrison DG (1997). Cellular and molecular mechanisms of endothelial cell dysfunction. J Clin Invest 100: 2153–2157.

Hollinger S, Hepler JR (2002). Cellular regulation of RGS proteins: modulators and integrators of G protein signaling. Pharmacol Rev 54: 527–559.

Iiyama K, Hajra L, Iiyama M, Li H, DiChiara M, Medoff BD *et al*. (1999). Patterns of vascular cell adhesion molecule-1 and intercellular adhesion molecule-1 expression in rabbit and mouse atherosclerotic lesions and at sites predisposed to lesion formation. Circ Res 85: 199–207.

Jiang DS, Wei X, Zhang XF, Liu Y, Zhang Y, Chen K *et al*. (2014). IRF8 suppresses pathological cardiac remodelling by inhibiting calcineurin signalling. Nat Commun 5: 3303.

Jin Y, An X, Ye Z, Cully B, Wu J, Li J (2009). RGS5, a hypoxia-inducible apoptotic stimulator in endothelial cells. J Biol Chem 284: 23436–23443.

Kilkenny C, Browne W, Cuthill IC, Emerson M, Altman DG (2010). Animal research: reporting *in vivo* experiments: the ARRIVE guidelines. Br J Pharmacol 160: 1577–1579.

Kirsch T, Wellner M, Luft FC, Haller H, Lippoldt A (2001). Altered gene expression in cerebral capillaries of stroke-prone spontaneously hypertensive rats. Brain Res 910: 106–115.

Kolodgie FD, Virmani R, Burke AP, Farb A, Weber DK, Kutys R *et al*. (2004). Pathologic assessment of the vulnerable human coronary plaque. Heart 90: 1385–1391.

Kyriakis JM, Avruch J (2001). Mammalian mitogen-activated protein kinase signal transduction pathways activated by stress and inflammation. Physiol Rev 81: 807–869.

Kyriakis JM, Avruch J (2012). Mammalian MAPK signal transduction pathways activated by stress and inflammation: a 10-year update. Physiol Rev 92: 689–737.

Ley K, Laudanna C, Cybulsky MI, Nourshargh S (2007). Getting to the site of inflammation: the leukocyte adhesion cascade updated. Nat Rev Immunol 7: 678–689.

Li H, He C, Feng J, Zhang Y, Tang Q, Bian Z *et al*. (2010). Regulator of G protein signaling 5 protects against cardiac hypertrophy and fibrosis during biomechanical stress of pressure overload. Proc Natl Acad Sci U S A 107: 13818–13823.

Li L, Chen W, Zhu Y, Wang X, Jiang DS, Huang F *et al*. (2014). Caspase Recruitment domain 6 protects against cardiac hypertrophy in response to pressure overload. Hypertension 64: 94–102.

Libby P (2002). Inflammation in atherosclerosis. Nature 420: 868–874.

Lloyd-Jones D, Adams RJ, Brown TM, Carnethon M, Dai S, De Simone G *et al*. (2010). Executive summary: heart disease and stroke statistics – 2010 update: a report from the American Heart Association. Circulation 121: 948–954.

Lu J, Bian ZY, Zhang R, Zhang Y, Liu C, Yan L *et al*. (2013). Interferon regulatory factor 3 is a negative regulator of pathological cardiac hypertrophy. Basic Res Cardiol 108: 326.

Mallat Z, Besnard S, Duriez M, Deleuze V, Emmanuel F, Bureau MF *et al*. (1999). Protective role of interleukin-10 in atherosclerosis. Circ Res 85: e17–e24.

McGrath J, Drummond G, McLachlan E, Kilkenny C, Wainwright C (2010). Guidelines for reporting experiments involving animals: the ARRIVE guidelines. Br J Pharmacol 160: 1573–1576.

Mestas J, Ley K (2008). Monocyte-endothelial cell interactions in the development of atherosclerosis. Trends Cardiovasc Med 18: 228–232.

Molkentin JD (2004). Calcineurin-NFAT signaling regulates the cardiac hypertrophic response in coordination with the MAPKs. Cardiovasc Res 63: 467–475.

Pawson AJ, Sharman JL, Benson HE, Faccenda E, Alexander SP, Buneman OP *et al*.; NC-IUPHAR (2014). The IUPHAR/BPS Guide to PHARMACOLOGY: an expert-driven knowledge base of drug targets and their ligands. Nucl. Acids Res. 42 (Database Issue): D1098–D1106.

Potteaux S, Deleuze V, Merval R, Bureau MF, Esposito B, Scherman D *et al*. (2006). *In vivo* electrotransfer of interleukin-10 cDNA prevents endothelial upregulation of activated NF-kappaB and adhesion molecules following an atherogenic diet. Eur Cytokine Netw 17: 13–18.

Rosenfeld ME, Carson KG, Johnson JL, Williams H, Jackson CL, Schwartz SM (2002). Animal models of spontaneous plaque rupture: the holy grail of experimental atherosclerosis research. Curr Atheroscler Rep 4: 238–242.

Ross R (1999). Atherosclerosis – an inflammatory disease. N Engl J Med 340: 115–126.

Stary HC, Chandler AB, Dinsmore RE, Fuster V, Glagov S, Insull W Jr *et al*. (1995). A definition of advanced types of atherosclerotic lesions and a histological classification of atherosclerosis. A report from the Committee on Vascular Lesions of the Council on Arteriosclerosis, American Heart Association. Arterioscler Thromb Vasc Biol 15: 1512–1531.

Surapisitchat J, Hoefen RJ, Pi X, Yoshizumi M, Yan C, Berk BC (2001). Fluid shear stress inhibits TNF-alpha activation of JNK but not ERK1/2 or p38 in human umbilical vein endothelial cells: inhibitory crosstalk among MAPK family members. Proc Natl Acad Sci U S A 98: 6476–6481.

Tabas I (2005). Consequences and therapeutic implications of macrophage apoptosis in atherosclerosis: the importance of lesion stage and phagocytic efficiency. Arterioscler Thromb Vasc Biol 25: 2255–2264.

Tabas I (2010). Macrophage death and defective inflammation resolution in atherosclerosis. Nat Rev Immunol 10: 36–46.

Virmani R, Burke AP, Kolodgie FD, Farb A (2002). Vulnerable plaque: the pathology of unstable coronary lesions. J Interv Cardiol 15: 439–446.